Nuclear Inst. and Methods in Physics Research, A 1042 (2022) 167394

Contents lists available at ScienceDirect

Nuclear Inst. and Methods in Physics Research, A

journal homepage: www.elsevier.com/locate/nima

Technical notes

# Stability control method of double crystal monochromator based on hybrid control algorithm

Yang Bai [a,b], Xuepeng Gong [a,*], Qipeng Lu [a,*], Yuan Song [a], Wanqian Zhu [c], Song Xue [c], Dazhuang Wang [a], Zhongqi Peng [a], Zhen Zhang [a]

[a] State key Laboratory of Applied Optics, Changchun Institute of Optics, Fine Mechanics and Physics, Chinese Academy of Sciences, Changchun 130033, China
[b] University of Chinese Academy of Sciences, Beijing 100049, China
[c] Shanghai Advanced Research Institute, Chinese Academy of Sciences, Shanghai 201204, China

ARTICLE INFO

*Keywords:*
Synchrotron radiation
Double-crystal monochromator
Active vibration control
Hybrid control algorithm

ABSTRACT

The Bragg angle stability of the DCM (double crystal monochromator) in synchrotron radiation facilities is critical for beam position, flux and resolution of hard X-ray beam lines. Generally, the vibration caused by $LN_2$ cooling system is the most critical factor affecting the stability of DCM. In this paper, aiming at the stability of DCM, we propose the stability control method of double crystal monochromator base on hybrid control algorithm. The numerical results show that the stability of the DCM in the pitch direction can be greatly improved by this active vibration control method under $LN_2$ mode. The angular displacement RMS value in the pitch direction decreased from about 358.52 nrad to about 0.071nrad, which decreased by 99.98%. Proposed method is of great significance to the research of ultra-high stability DCM in synchrotron radiation facilities all over the world.

## 1. Introduction

Synchrotron radiation light source has become an advanced and irreplaceable tool for basic and applied research in the fields of materials science, life science, physics, chemistry, medicine and so on. Shanghai Synchrotron Radiation Facility (SSRF) is the third-generation synchrotron radiation light source in Chinese Mainland, which provides an advanced experimental platform for multidisciplinary frontier research and high-tech development and application.

Crystal monochromator is one of the most critical optical devices in the beam line of synchrotron, which directly affects the quality of beam energy and position. In recent years, in the field of synchrotron radiation, the stability of DCM will become the main technical bottleneck of the overall performance of many X-ray beams. With the continuous improvement of user requirements and considering the specific conditions of the optical system, the stability requirement of the actual DCM in the pitch direction is 30 ~50 nrad [1]. Generally, the angular stability of the 2nd crystal of the DCM in pitch direction has the greatest impact on the quality of the beam flux, position and resolution [2]. The vibration of DCM is mainly caused by the interference of the $LN_2$ circulating cooling system [3]. At present, in the field of synchrotron radiation, the stability of DCM is mainly guaranteed by passive vibration control, which optimizes the structure of cooling system or the mechanical structure of monochromator. The Japanese Spring-8 light source has designed a low vibration flexible tube, which stabilizes the coolant flow by covering the ripple of the flexible tube with alumina fiber fabric. At the same time, the cooling pipeline of the 2nd crystal is upgraded, which can theoretically improve the stability of the crystal to 50nrad [4]. ESRF proposes a new generation of mirror system that can be used to suppress vibration and ensure ultra-high thermal stability [5,6]. P2 protein crystallography beam line of SSRF optimizes the 2nd crystal attitude fine-tuning mechanism of DCM and the $LN_2$ cooling system. The stability in the pitch direction meets the 300nrad/2 h stability requirements in the user experiment of macromolecular crystallography beam line (P2-BL10U2) [7,8]. The 2nd crystal attitude fine-tuning mechanism of P2 protein crystallography beam line of SSRF is shown in Fig. 1.and the optimized four-axis flexure hinge is shown in Fig. 2.

In this paper, aiming at the micro-vibration problem of DCM of P2 experimental station of SSRF, the flexure hinge of the 2nd crystal fine-tuning mechanism is taken as the research object. The AVC (active vibration control) system is designed based on Feedback FxNLMS-Fuzzy PD algorithm. The results show that the active vibration control method based on Feedback FxNLMS-Fuzzy PD algorithm can greatly suppress the amplitude in the pitch direction of DCM. In particular, the angular displacement in the pitch direction can reach 0.071nrad. Therefore, this active vibration control method based on Feedback FxNLMS-Fuzzy PD algorithm provides an innovative technical scheme for upgrading the DCM of P2 experimental station of SSRF. It is of great significance for

* Corresponding authors.
*E-mail addresses:* gongxuepeng120@foxmail.com (X. Gong), luqipeng@126.com (Q. Lu).

https://doi.org/10.1016/j.nima.2022.167394
Received 1 August 2022; Received in revised form 9 August 2022; Accepted 15 August 2022
Available online 31 August 2022

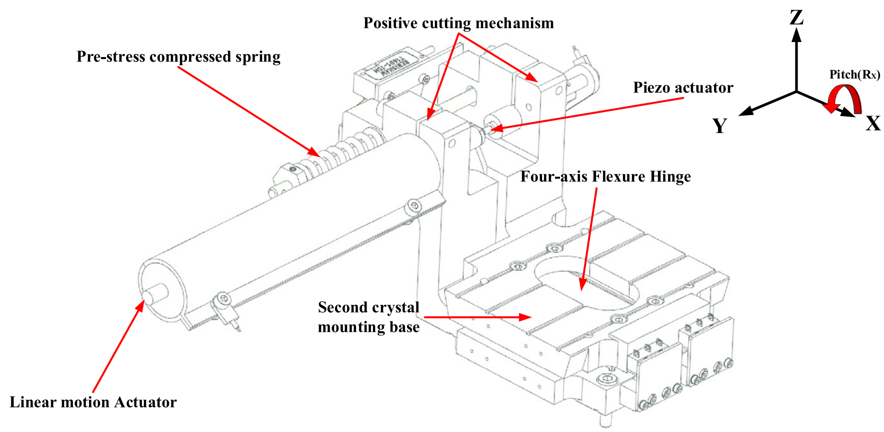


**Fig. 1.** Mechanism for the fine-tune along pitch direction of 2nd crystal.

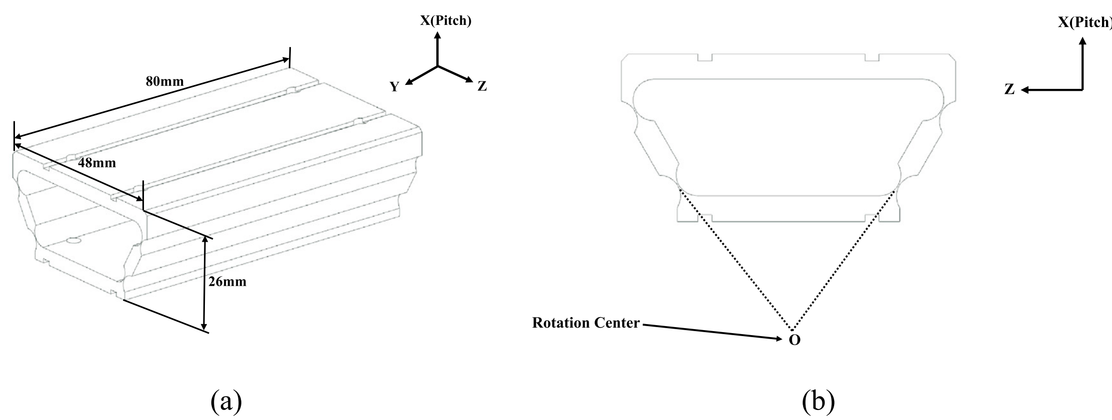


**Fig. 2.** Four-axis flexure hinge structure.

the development of ultra-high stable DCM in X-ray beam line stations of synchrotron radiation facilities all over the world.

## 2. Experimental setup

### 2.1. Dynamic analysis of four-axis flexure hinge

Select the generalized coordinate $\mathbf{q_j}$ $(\mathbf{j} = \mathbf{1}, \mathbf{2}, \cdots, \mathbf{n})$, the motion equation of four-axis flexure hinge can be described by the second type of Lagrange equation as follows:

$$\frac{\mathbf{d}}{\mathbf{dt}}\left(\frac{\partial \mathbf{T}}{\partial \dot{\mathbf{q}}_\mathbf{j}}\right) - \frac{\partial \mathbf{T}}{\partial \mathbf{q_j}} = \mathbf{Q_j} \tag{1}$$

$$\mathbf{Q_j} = -\frac{\partial \mathbf{U}}{\partial q_j} \tag{2}$$

Where $\mathbf{T}$ is the kinetic energy of the four-axis hinge system, $\dot{q}_j$ $(\mathbf{j} = \mathbf{1}, \mathbf{2}, \cdots, \mathbf{n})$ is the generalized velocity, $\mathbf{Q_j}$ $(\mathbf{j} = \mathbf{1}, \mathbf{2}, \cdots, \mathbf{n})$ is the generalized force in generalized coordinates, $\mathbf{U}$ is the potential energy of four-axis flexure hinge system.

$$\mathbf{U} = \frac{\mathbf{1}}{\mathbf{2}}\begin{bmatrix}\mathbf{q_1}\\ \vdots \\ \mathbf{q_n}\end{bmatrix}^\mathbf{T}\left[\begin{bmatrix}K_{11} & \cdots & K_{1n}\\ \vdots & \ddots & \vdots\\ K_{n1} & \cdots & K_{nn}\end{bmatrix}\right]\begin{bmatrix}\mathbf{q_1}\\ \vdots \\ \mathbf{q_n}\end{bmatrix} \tag{3}$$

Where $[\mathbf{q}]$ and $[\mathbf{q}]^\mathbf{T}$ are the generalized coordinate matrix and its transpose matrix respectively, $[\mathbf{K}]$ is the generalized stiffness matrix.

$$\mathbf{T} = \frac{\mathbf{1}}{\mathbf{2}}\begin{bmatrix}\dot{\mathbf{q}}_\mathbf{1}\\ \vdots \\ \dot{\mathbf{q}}_\mathbf{n}\end{bmatrix}^\mathbf{T}\left[\begin{bmatrix}m_{11} & \cdots & m_{1n}\\ \vdots & \ddots & \vdots\\ m_{n1} & \cdots & m_{nn}\end{bmatrix}\right]\begin{bmatrix}\dot{\mathbf{q}}_\mathbf{1}\\ \vdots \\ \dot{\mathbf{q}}_\mathbf{n}\end{bmatrix} \tag{4}$$

Where $[\dot{\mathbf{q}}]$ and $[\dot{\mathbf{q}}]^\mathbf{T}$ is the generalized velocity matrix and its transposition matrix, $[\mathbf{m}]$ is the generalized mass matrix. For damped forced vibration, Rayleigh dissipation function $\mathbf{D}$:

$$\mathbf{D} = \frac{\mathbf{1}}{\mathbf{2}}[\dot{\mathbf{q}}]^\mathbf{T}[\mathbf{C}][\dot{\mathbf{q}}] \tag{5}$$

Where $[\mathbf{C}]$ is the damping matrix.

Then the matrix form of the differential equation of system dynamics is:

$$[\mathbf{m}][\ddot{q}] + [\mathbf{C}][\dot{\mathbf{q}}] + [\mathbf{K}][\mathbf{q}] = [\tilde{Q}] \tag{6}$$

Where $[\tilde{Q}]$ is a non-force matrix except damping.

Based on the above theory, through Adams-MATLAB joint analysis and calculation, the frequency response function curve of the flexure hinge is shown in Fig. 3. In the full frequency range, the natural frequency of the four-axis flexure hinge is 452 Hz. The modal participation factors in different directions of the four-axis flexure hinge are shown in Fig. 4. It can be seen that under the same excitation conditions, the mode in the pitch direction contributes the most to the response.

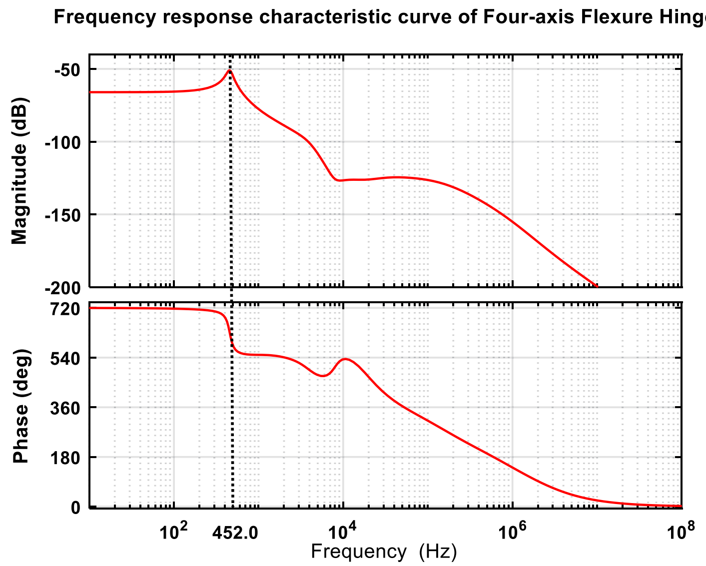


**Fig. 3.** Frequency response curve of four axis flexure hinge.

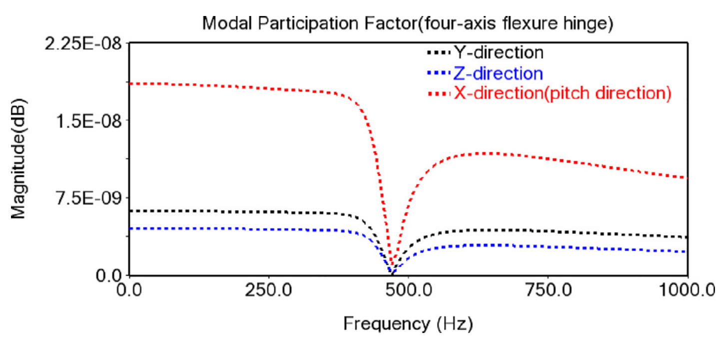


**Fig. 4.** Modal participation factor in X/Y/Z direction.

### 2.2. Design of AVC system

The Feedback FxNLMS (filter-X normalized least mean square) algorithm does not need external interference related reference signals, which is driven by residual error signals. Feedback FxNLMS algorithm has the characteristics of good effect, strong adaptability and easy engineering implementation. It is widely used in the field of active vibration control. The control system based on Feedback FxNLMS algorithm uses residual error signal to drive the control system, which convergence accuracy will be disturbed by the residual error signal. Generally, the influence of the residual error signal on the convergence accuracy of the system can be reduced by changing the iteration step-size. However, changing the iteration step size will affect the convergence speed of the control system [9,10]. When the nonlinearity of the system and the system parameters fluctuate greatly with external interference, the composite controller based on Fuzzy PD algorithm can enhance the adaptability to environmental changes by changing the parameters of PD controller online. Thus, it can not only ensure the dynamic response effect, but also improve the steady-state control accuracy, so that the comprehensive control effect of the system is excellent. The basic structure of the control system based on the Feedback FxNLMS-Fuzzy PD algorithm is shown in Fig. 5, the schematic diagram of the adaptive Fuzzy-PD controller is shown in Fig. 6.

The calculation formula of the control system based on Feedback FxNLMS-Fuzzy PD algorithm is as follows:

$$\mathbf{x}(\mathbf{n}) = \mathbf{e}(\mathbf{n}) + \mathbf{S}'(\mathbf{n}) * \mathbf{y}(\mathbf{n}) \tag{7}$$

$$\mathbf{e}(\mathbf{n}) = \mathbf{d}(\mathbf{n}) + \mathbf{y_s}(\mathbf{n}) \tag{8}$$

$$\mathbf{U_1}(\mathbf{n}) = \mathbf{w^T}(\mathbf{n})\,\mathbf{x}(\mathbf{n}) \tag{9}$$

$$\mathbf{U_2}(\mathbf{n}) = \mathbf{K_P} \cdot \mathbf{e}(\mathbf{n}) + \mathbf{K_D}\frac{\mathbf{N}}{\mathbf{1} + \mathbf{N} \cdot \mathbf{T_s}\frac{\mathbf{1}}{\mathbf{z-1}}} \cdot \mathbf{e}(\mathbf{n}) \tag{10}$$

$$\mathbf{K_P} = \mathbf{K_{P0}} + \Delta\mathbf{K_P} \tag{11}$$

$$\mathbf{K_D} = \mathbf{K_{D0}} + \Delta\mathbf{K_D} \tag{12}$$

$$\mathbf{y}(\mathbf{n}) = \mathbf{U_1}(\mathbf{n}) + \mathbf{U_2}(\mathbf{n}) \tag{13}$$

$$\mathbf{w}(\mathbf{n+1}) = \mathbf{w}(\mathbf{n}) + \frac{\tilde{\mu}}{\delta + \|\mathbf{x}(\mathbf{n})\|^2}\mathbf{x}(\mathbf{n})\mathbf{e}(\mathbf{n}) \tag{14}$$

Where $\mathbf{e}(\mathbf{n})$ is the residual error signal, $\mathbf{S}'(\mathbf{n})$ is the estimation of the secondary channel, $\mathbf{y}(\mathbf{n})$ is the output of Feedback FxNLMS-Fuzzy PD control system, $\mathbf{d}(\mathbf{n})$ is the original vibration signal, $\mathbf{y_s}(\mathbf{n})$ is the anti-vibration signal, $\mathbf{U_1}(\mathbf{n})$ is the Feedback FxNLMS control system output, $\mathbf{U_2}(\mathbf{n})$ is the output of Fuzzy-PD controller, $\mathbf{K_P}$, $\mathbf{K_D}$ is the set proportional and differential coefficients under fuzzy rules, $\mathbf{K_{P0}}$ is the initial proportion parameter, $\mathbf{K_{D0}}$ is the initial differential parameter, $\mathbf{N}$ is the filter coefficient of PD controller, $\mathbf{T_s}$ is discrete time, $\mathbf{w}(\mathbf{n})$ is the iterative weight of Feedback FxNLMS controller, $\tilde{\mu}$ iteration step-size, $\delta$ is a constant.

The variation range of error $\mathbf{e}$ and error variation $\mathbf{ec}$ is defined as the universe on the fuzzy set:

$$\mathbf{e}, \mathbf{ec} = \{-\mathbf{300}, -\mathbf{200}, -\mathbf{100}, \mathbf{0}, \mathbf{100}, \mathbf{200}, \mathbf{300}\} \tag{15}$$

The fuzzy subsets are:

$$\mathbf{e}, \mathbf{ec} = \{\mathbf{NB}, \mathbf{NM}, \mathbf{NS}, \mathbf{ZO}, \mathbf{PS}, \mathbf{PM}, \mathbf{PB}\} \tag{16}$$

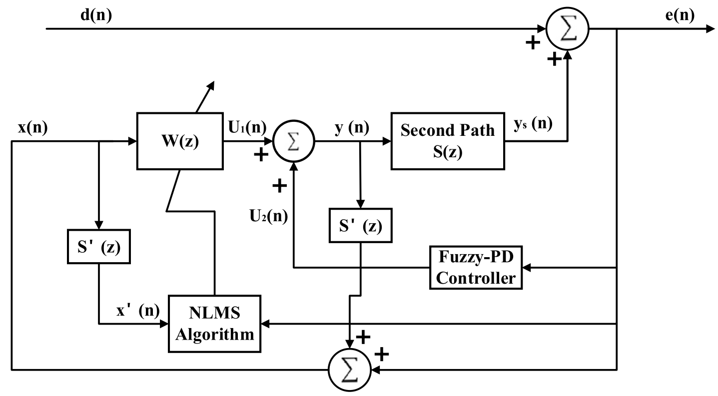


**Fig. 5.** Basic structure of control system based on Feedback FxNLMS-Fuzzy PD algorithm.

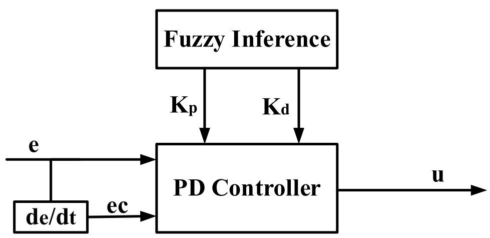


**Fig. 6.** Schematic diagram of adaptive Fuzzy-PD controller.

**Table 1**
The work frequency of DCM in P2 experimental station of SSRF at Bragg@12.66kev.

| Operating Mode | Frequency (Hz) | | | | |
|---|---|---|---|---|---|
| Before $LN_2$ | 38.15 | 51.67 | 84.60 | 90.03 | 108.20 |
| After $LN_2$ | 38.38 | 51.60 | 64.30 | – | – |

## 3. Results and discussions

The work frequency of DCM in P2 experimental station of SSRF at Bragg@12.66 kev is shown in Table 1 [11]. The time-domain curve of vibration source is shown in Fig. 7 and the frequency-domain curve of vibration source is shown in Fig. 8.

### 3.1. Time-domain analysis

The time-domain results of the four-axis flexure hinge in pitch direction linear displacement signal at Bragg@12.66 kev are shown in Fig. 9. The RMS value of flexure hinge angular displacement in pitch direction is shown in Table 2. The active vibration control method makes the angular displacement of flexure hinge in pitch direction decrease obviously. In particular, the vibration reduction effect of feedback FxNLMS-Fuzzy PD is better than feedback FxNLMS algorithm and feedback FxNLMS-PD algorithm. The angular displacement of the flexure hinge in pitch direction can be reduced by 99.41% at most without $LN_2$ cooling. On the other hand, the angular displacement of the flexure hinge in pitch direction can be reduced by 99.98% at most with $LN_2$ cooling.

### 3.2. Frequency-domain analysis

The frequency-domain results of the four-axis flexure hinge in pitch direction displacement signal at Bragg@12.66 kev are shown in Fig. 10. In particular, PSD values at work frequency and natural frequency before and after $LN_2$ cooling are shown in Tables 3 and 4 respectively. Obviously, in the frequency range of 0 ~500 Hz, with the active vibration control method, the PSD value of displacement in pitch direction generally shows an obvious downward trend and the displacement signal energy is greatly weakened. In particular, the Feedback FxNLMS-fuzzy PD control method is the most effective. With the Feedback FxNLMS-Fuzzy PD control method, the PSD value at the natural frequency of 452 Hz decreases by 61.776 dBm/Hz without $LN_2$ cooling, which is about 62.10%. On the other hand, with the Feedback FxNLMS-Fuzzy PD control method, the PSD value at the natural frequency of 452 Hz decreases by 69.814 dBm/Hz with $LN_2$ cooling, which is about 81.66%.

**Table 2**
RMS value of angular displacement of four-axis flexure hinge in pitch direction at Bragg@12.66kev.

| Method | Uncontrolled | Feedback FxNLMS | Feedback FxNLMS-PD | Feedback FxNLMS-Fuzzy PD |
|---|---|---|---|---|
| Before $LN_2$ | 75.14 nrad | 7.32 nrad | 1.29 nrad | 0.044 nrad |
| After $LN_2$ | 358.52 nrad | 64.49 nrad | 0.76 nrad | 0.071 nrad |

**Table 3**
PSD values of four-axis flexure hinge in pitch direction without $LN_2$ cooling at Bragg@12.66kev.

| Frequency (Hz) | Uncontrolled (dBm/Hz) | Feedback FxNLMS (dBm/Hz) | Feedback FxNLMS-PD (dBm/Hz) | FxNLMS-Fuzzy PD (dBm/Hz) |
|---|---|---|---|---|
| 38.15 | −110.556 | −165.071 | −165.264 | −183.856 |
| 51.67 | −110.583 | −160.010 | −160.110 | −181.328 |
| 84.60 | −121.858 | −167.043 | −171.262 | −190.458 |
| 90.03 | −119.071 | −161.474 | −166.905 | −186.276 |
| 108.20 | −109.461 | −146.614 | −154.357 | −173.986 |
| 452.00 | −99.477 | −118.681 | −133.770 | −161.253 |

**Table 4**
PSD values of four-axis flexure hinge in pitch direction with $LN_2$ cooling at Bragg@12.66kev.

| Frequency (Hz) | Uncontrolled (dBm/Hz) | Feedback FxNLMS (dBm/Hz) | Feedback FxNLMS-PD (dBm/Hz) | FxNLMS-Fuzzy PD (dBm/Hz) |
|---|---|---|---|---|
| 38.38 | −95.456 | −149.317 | −150.632 | −182.212 |
| 51.60 | −97.951 | −149.614 | −151.626 | −183.446 |
| 64.30 | −98.409 | −143.133 | −148.294 | −180.550 |
| 452.00 | −85.493 | −99.874 | −153.248 | −155.307 |

### 3.3. Short-time Fourier analysis

The Fourier transform only reflects the characteristics of the signal in frequency-domain and cannot analyze the signal in time-domain. Short-time Fourier transform is used for spectrum analysis of slow time-varying signals, which represents the signal characteristics at a certain

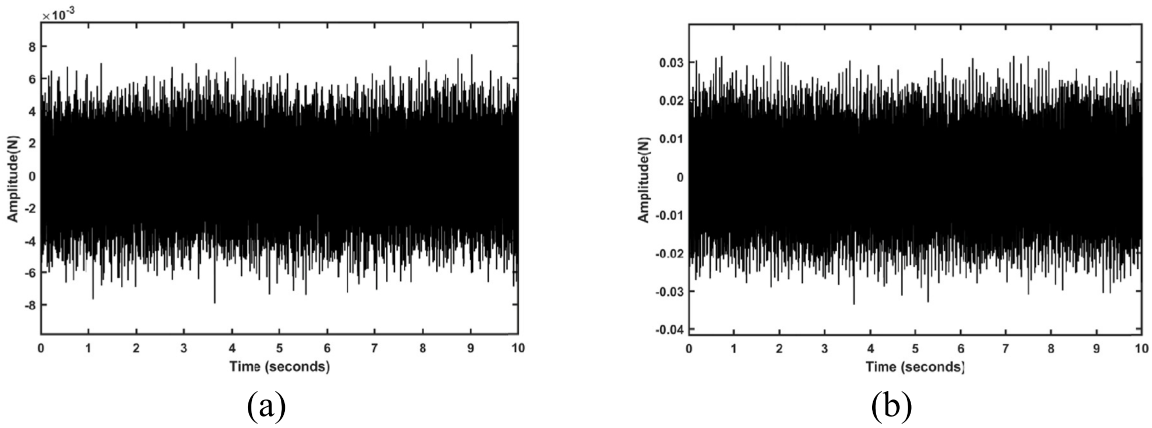


**Fig. 7.** Time-domain curve of vibration source. (a) before $LN_2$ cooling (b) after $LN_2$ cooling.

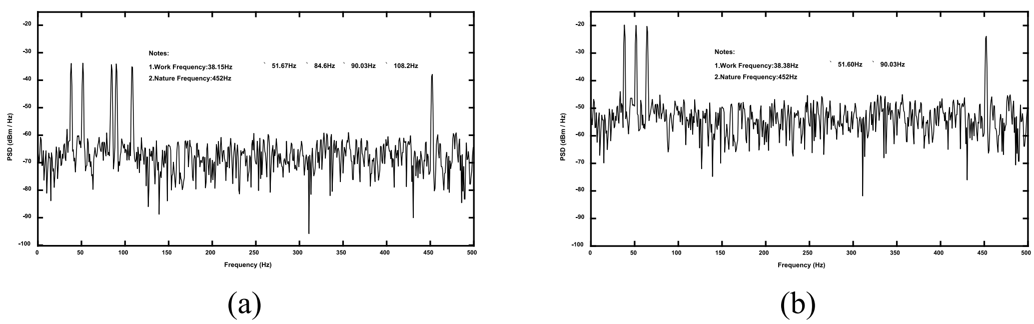


**Fig. 8.** Frequency-domain curve of vibration source. (a) before $LN_2$ cooling (b) after $LN_2$ cooling.

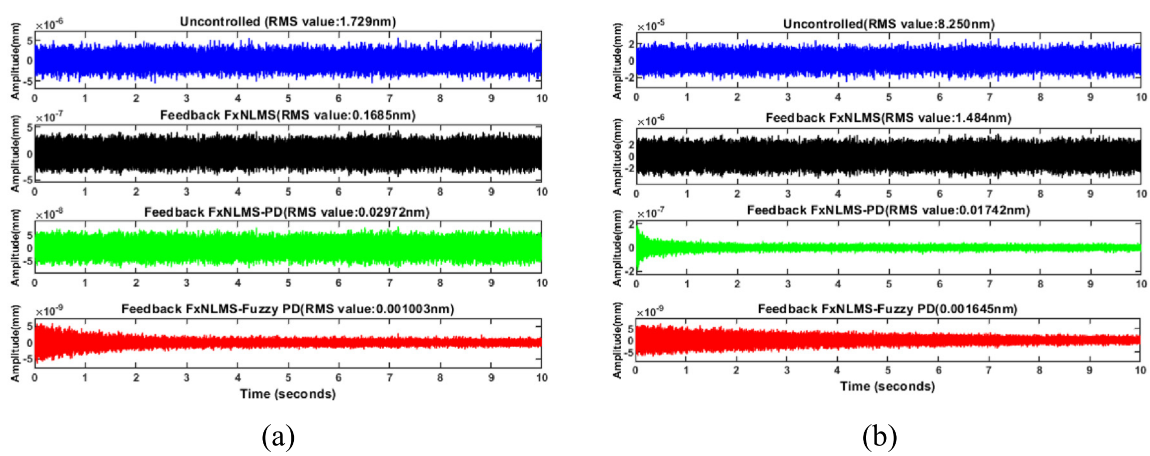


**Fig. 9.** The time-domain results of the four-axis flexure hinge in pitch direction linear displacement signal at Bragg@12.66kev. (a) before $LN_2$ cooling (b) after $LN_2$ cooling.

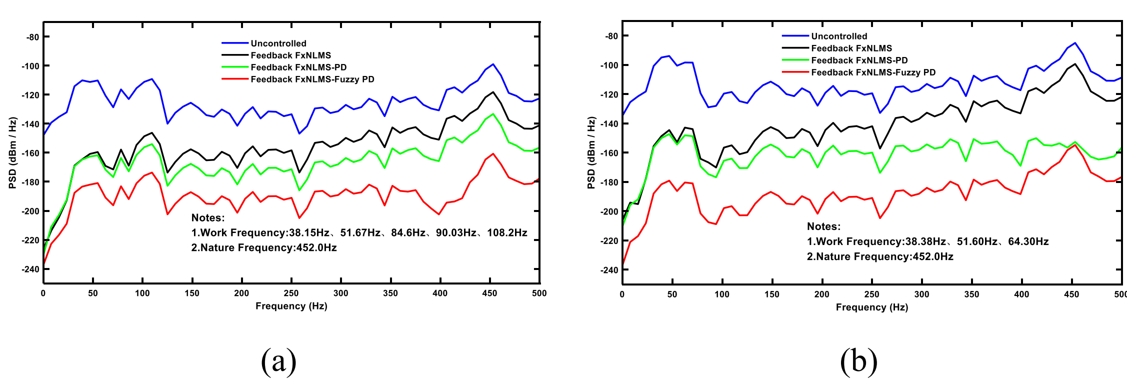


**Fig. 10.** The Frequency-domain results of the four-axis flexure hinge in pitch direction linear displacement signal at Bragg@12.66kev. (a) before $LN_2$ cooling (b) after $LN_2$ cooling.

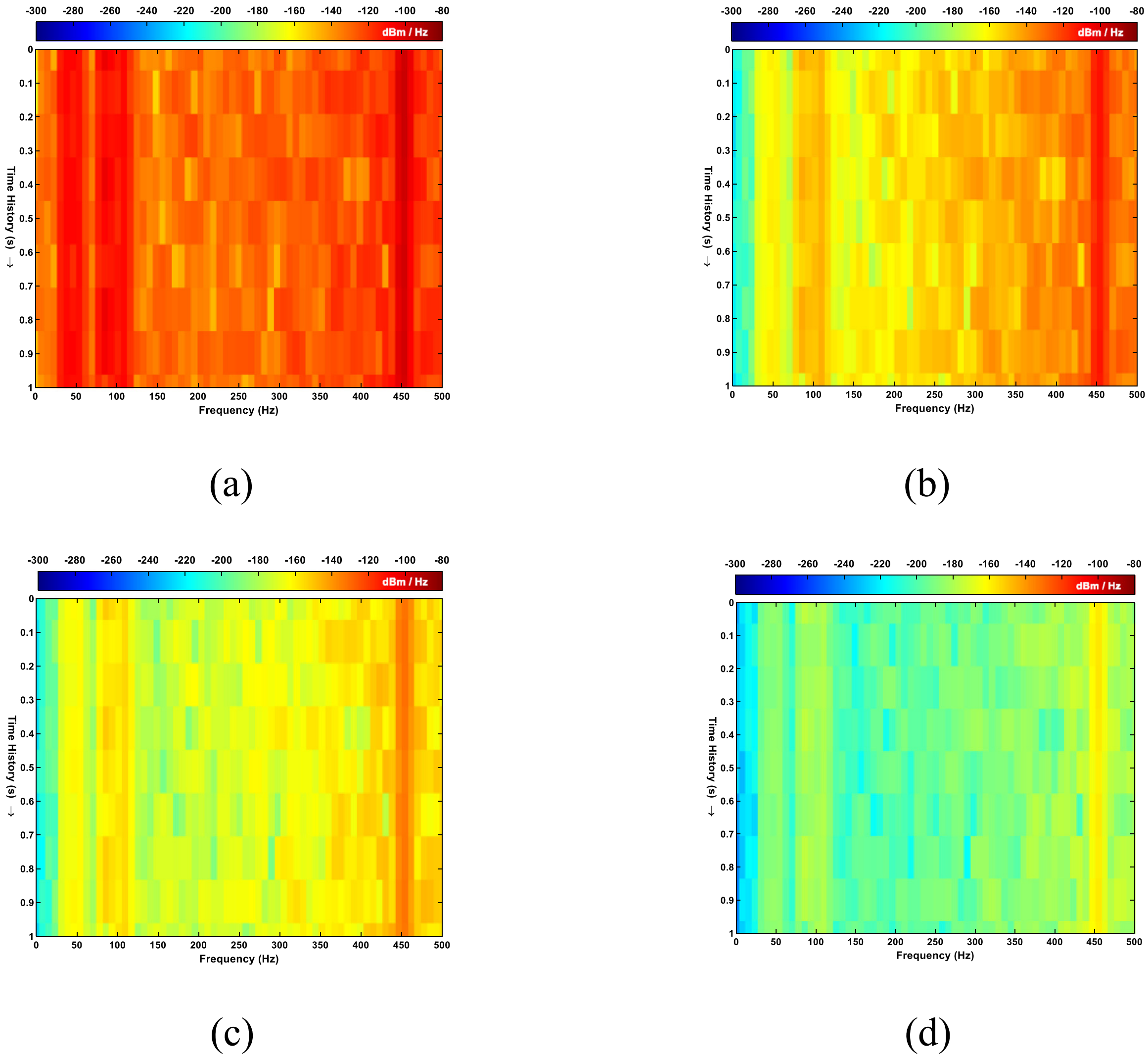


**Fig. 11.** The short-time Fourier analysis results of the four-axis flexure hinge in pitch direction displacement signal at Bragg@12.66kev without $LN_2$ cooling. (a) Uncontrolled (b) Feedback FxNLMS (c) Feedback FxNLMS-PD (d) Feedback FxNLMS-Fuzzy PD.

time through a signal in the time window. The time-varying spectrum signal can be observed by short-time Fourier transform. Short-time Fourier transform can not only make up for the shortcoming of observing time in spectrum analysis, but also make up for the shortcoming of obtaining frequency in time-domain analysis. The short-time Fourier transform of signal $\mathbf{x(t)}$ at time $\mathbf{t}$ is:

$$\mathbf{STFT}\,(\mathbf{t},\mathbf{f}) = \int_{-\infty}^{\infty} \mathbf{x}\,(\tau)\,\mathbf{h}(\tau-\mathbf{t})\mathbf{e}^{-\mathbf{j}2\pi\mathbf{f}\tau}\mathbf{d}\tau \tag{17}$$

Where $\mathbf{h}\,(\tau-\mathbf{t})$ is the analysis window function.

Based on the above basic principles, the short-time Fourier analysis results of the four-axis flexure hinge in pitch direction displacement signal at Bragg@12.66 kev without $LN_2$ cooling are shown in Fig. 11, the short-time Fourier analysis results of the four-axis flexure hinge in pitch direction displacement signal at Bragg@12.66 kev with $LN_2$ cooling are shown in Fig. 12. On the whole, it can be intuitively analyzed that the amplitude of displacement signal corresponding to Uncontrolled, Feedback FxNLMS control method, Feedback FxNLMS-PD control method and Feedback FxNLMS-Fuzzy PD control method decreases in turn. Before and after $LN_2$ cooling, the color gradually becomes lighter at the working frequency and the signal amplitude is greatly attenuated. In particular, before and after $LN_2$ cooling, the resonant peak at the frequency of 452 Hz has a significant attenuation effect. Among them, the Feedback FxNLMS-Fuzzy PD control method has the best effect.

## 4. Conclusions

Aiming at the micro-vibration problem of the crystal attitude fine-tuning mechanism of the DCM, this paper takes the flexure hinge of the 2nd crystal attitude fine-tuning mechanism of the P2 beamline at SSRF as the research object and proposes a new active vibration control method based on the Feedback FxNLMS-Fuzzy PD algorithm. With the active vibration control method based on Feedback FxNLMS-Fuzzy PD algorithm, the RMS value angular displacement of four-axis flexure hinge in pitch direction can be reduced to 0.071nrad. In particular, PSD values at work frequency and natural frequency before and after $LN_2$ cooling decreases significantly. Similarly, through short-time Fourier analysis, the active control method based on Feedback FxNLMS-Fuzzy PD algorithm shows ideal vibration reduction effect. It can be seen that the active control method is effective and can ensure the stability index of the DCM under $LN_2$ cooling condition.

It is worth noting that the active control method can theoretically control the angular displacement RMS value of flexure hinge in pitch direction below about 0.1nrad. In particular, this paper simulates and analyzes the key components of the second crystal mechanism and proposes a novel hybrid control algorithm, while the actual monochromator stability index needs further experimental verification and engineering exploration in future.

This stability control method based on Feedback FxNLMS-Fuzzy PD algorithm not only provides a new technical scheme for upgrading

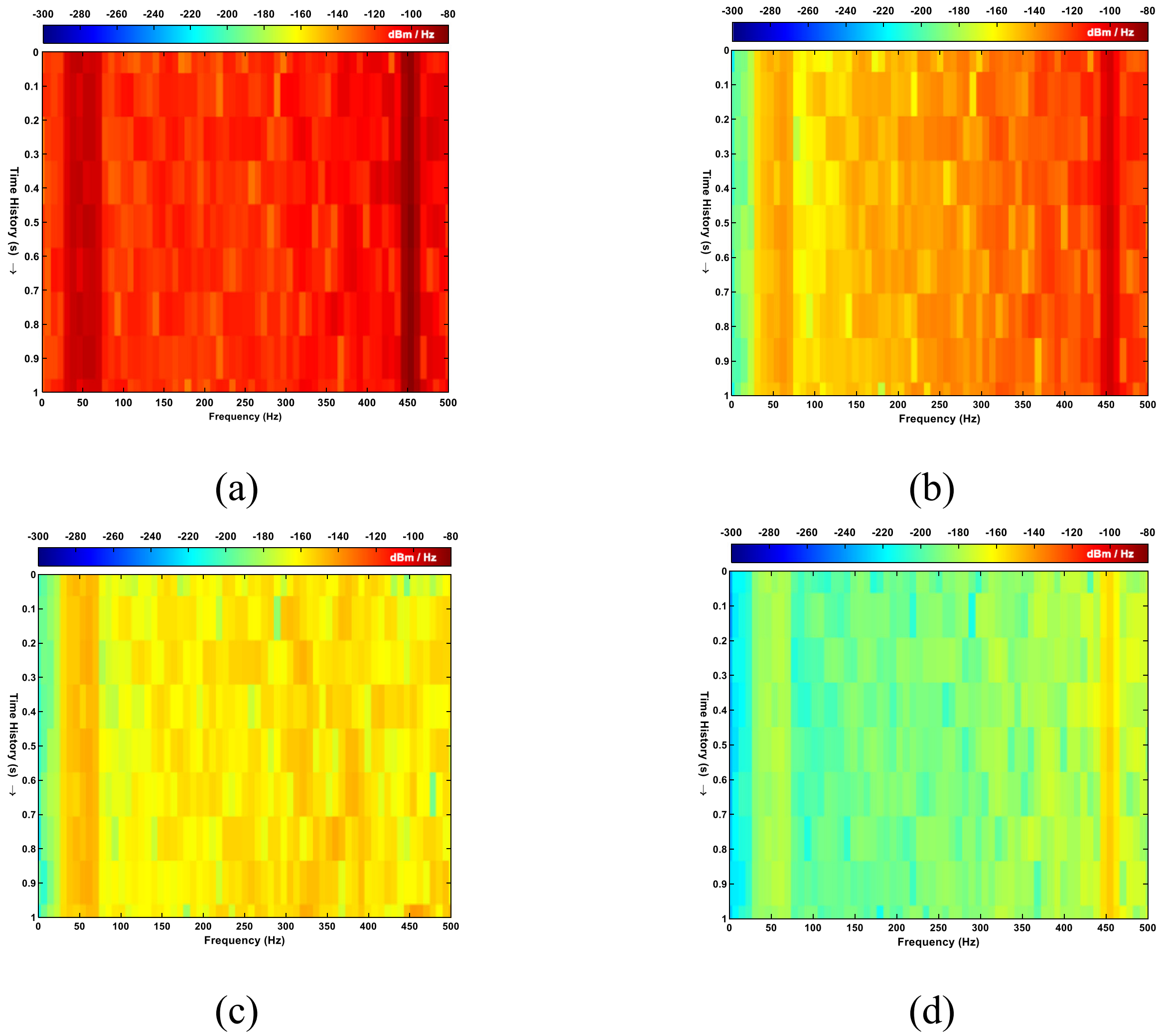


**Fig. 12.** The short-time Fourier analysis results of the four-axis flexure hinge in pitch direction displacement signal at Bragg@12.66kev with $LN_2$ cooling. (a) Uncontrolled (b) Feedback FxNLMS (c) Feedback FxNLMS-PD (d) Feedback FxNLMS-Fuzzy PD.

the DCM of P2 experimental station of SSRF, but also has extremely important reference value for synchrotron radiation facilities all over the world to study the ultra-high stability DCM.

## Declaration of competing interest

The authors declare that they have no known competing financial interests or personal relationships that could have appeared to influence the work reported in this paper.

## Data availability

The authors do not have permission to share data.

## Acknowledgments

The work is supported by National Natural Science Foundation of China (No. 61974142, No. 62104224) and "Xu-Guang" Talent Program of Changchun Institute of Optics, Fine Mechanics and Physics (CIOMP), Chinese Academy of Sciences (CAS) (E01672Y6Q0). Thanks to the support of the researchers at SSRF (Shanghai Synchrotron Radiation Facilities of China).

## References

[1] Preliminary design report of SSRF beamline project(phaseII), 2017, p. 4.
[2] Yichen Fan, et al., Angular stability measurement of a cryocooled double-crystal monochromator at SSRF, Nucl. Inst. Methods Phys. Res. 983 (2020) 164636.
[3] R.M. Galiari, et al., Studies on flow-include-vibration for the new high-dynamics DCM for sirius presented at MEDSI 2016, 2016, Barcelona, Spain.
[4] Hiroshi Yamazaki, et al., Challenges toward 50 nrad-stability of x-rays for a next generation light source by refinements of spring-8 standard monochromator with cryo-cooled si crystals, in: AIP Conference Proceedings 2054, 2019, p. 060018.
[5] Roland Barrett, et al., New generation mirror systems for the ESRF upgrade beam lines, J. Phys. Conf. Series (2013).
[6] Y. Dabin, L. Zhang, D. Martin, et al., The concrete slab studies for the ESRF upgrade beamlines, in: The 7th International Conference on Mechanical Engineering Design of Synchrotron Radiation Equipment and Instrumentation, Vol. 2012, MEDSI, Shanghai, 2012.
[7] Wu Jiaxing, Gong Xuepeng, et al., Improvement of the performance of a cryo-cooled monochromator at SSRF.part I:Double-crystal parallelism, Nucl. Inst. Methods Phys. Res. (2021).
[8] Wu. Jiaxing, Gong Xuepeng, et al., Improvement of the performance of a cryo-cooled monochromator at ssrf.part II: Angular stability of the exit beam, Nucl. Inst. Methods Phys. Res. (2021).
[9] S.W. Gao, Q.Z. Huang, Z.Y. Gao, Active vibration control algorithm using reference signal self-extraction, J. Vib. Meas. Diagnosis 30 (5) (2010) 514–518.
[10] Weiguang Li, Zhichun Yang, Kui Li, Wei Wang, Hybrid feedback PID-FxLMS algorithm for active vibration control of cantilever beam with piezoelectric stack actuator, J. Sound Vib. 509 (2021) 116243.
[11] Stability test report of DCM in P2 beam line station of SSRF, 2020, p. 3.